A Multi-hypothesis Filter for Passive Tracking of Surface and Sub-Surface Target Localization

Wilbur J., Hyland J., Dobeck G. and Sermarini C.
Code HS13, NSWCPC West Hwy 98
Panama City Beach, FL 32408
joellen.wilbur@navy.mil

Abstract – **A Multi-hypothesis Iterated-Extended Kalman Filter (MHEKF) for passive sonar tracking and localization of surface and submerged targets using elevation and bearing angle measurements is presented. The MHEKF operates in a multi-depth mode by creating a bank of independently operating range-parameterized Cartesian EKFs, each receiving the same measurement data. The multi-depth mode operation allows the EKF to determine a unique *(x, y, z)* position solution using elevation and bearing measurements. At the first available measurement, the multi-hypothesis filter logic calculates the number and positioning of the depth banks in the water column from the operational decision radius along with the sensor beam widths and water depth. The bank depths are set in a geometric progression that yields constant coefficient of variation in range calculated with respect to the operational decision region. The MHEKF uses the normalized likelihood from each EKF depth-mode output to recursively update the target track. Any velocity or Doppler information available will reduce track ambiguity that arises when the tracker is expected to distinguish fast moving targets on the surface from slow moving targets at depth.**

I. INTRODUCTION

Passive detection tracking and localization of surface and submerged targets from angle-only measurements has wide application [1-6]. The application discussed in this paper focuses on passive tracking for bottom-mounted, influence type technology. These acoustic and magnetic sensors provide elevation and bearing measurements to targets. This paper addresses the problem of using non-periodic, noisy angle measurements from a sensor array to estimate and refine estimates of target position and speed in a fixed Cartesian coordinate system.

The classical approach has been to use the extended Kalman filter (EKF). We have built upon an iterated-extended Kalman filter model originated for passive tracking of surface and subsurface targets from bearing and elevation measurements [1]. The lack of range information was addressed by implementing a multi-depth mode Kalman filter. The multi-depth mode works by creating a family of filters for each target. Each filter in the family restricts the target's tracked depth to within prescribed limits by generating hypothetical range measurements centered in the corresponding depth interval; the variance of these range measurements is set very high.

The Multi-hypothesis Iterated-Extended Kalman Filter (MHEKF) creates a composite track where the probability of each model is calculated independently, then a multi-hypothesis estimate and covariance are calculated from a weighted sum of the individual output models [3,4,5,6]. Because the tracker remains in a fixed position the integration of target class or velocity information is needed for a unique solution [3,6]. That is, a unique solution from angle vectors necessitates the platform trajectory have one more nonzero derivative than does the target. Otherwise this additional information is needed for a unique mapping between the target parameters and the observation matrix.

II. MULTI-HYPOTHESIS KALMAN FILTER

The MHEKF operates in a multi-depth mode by creating a bank of independently operating range-parameterized Cartesian EKFs, each receiving the same measurement data. At the first available measurement the multi-hypothesis filter logic calculates the number and positioning of the depth banks in the water column from the operational decision radius along with the sensor beam widths and water depth. The depth modes are set in a geometric progression that determines the corresponding range parameters for each filter in the bank so that the coefficient of variation in range calculated with respect to the operational decision region is constant. The MHEKF uses the normalized likelihood from each EKF depth-mode output to recursively update the target track.

Multiple targets are tracked by creating a new multi-hypothesis filter for each target. The measurement/track matching logic computes the normalized residual error inner product test statistic from each MHEKF. This test statistic has a Chi-squared distribution [7,8] and is used to statistically compare new measurements to all existing target tracks.

A. Range Parameterization of the EKF Depth Modes

The filter depths in the multi-hypothesis filter are centered in depth intervals defined to follow a geometric progression. The filter bank order and depth intervals are automatically set by the MHEKF upon the first elevation measurement input. The filter depths are set in a geometric progression designed for a constant coefficient of variation in range calculated with respect to the operational decision region.

1-4244-0115-1/06/$20.00 ©2006 IEEE

Report Documentation Page

Form Approved
OMB No. 0704-0188

1. REPORT DATE	2. REPORT TYPE	3. DATES COVERED
01 SEP 2006	**N/A**	**-**

4. TITLE AND SUBTITLE	5a. CONTRACT NUMBER
A Multi-hypothesis Filter for Passive Tracking of Surface and Sub-Surface Target Localization	5b. GRANT NUMBER
	5c. PROGRAM ELEMENT NUMBER
6. AUTHOR(S)	5d. PROJECT NUMBER
	5e. TASK NUMBER
	5f. WORK UNIT NUMBER
7. PERFORMING ORGANIZATION NAME(S) AND ADDRESS(ES) **Code HS13, NSWCPC West Hwy 98 Panama City Beach, FL 32408**	8. PERFORMING ORGANIZATION REPORT NUMBER
9. SPONSORING/MONITORING AGENCY NAME(S) AND ADDRESS(ES)	10. SPONSOR/MONITOR'S ACRONYM(S)
	11. SPONSOR/MONITOR'S REPORT NUMBER(S)

12. DISTRIBUTION/AVAILABILITY STATEMENT
Approved for public release, distribution unlimited

13. SUPPLEMENTARY NOTES
See also ADM002006. Proceedings of the MTS/IEEE OCEANS 2006 Boston Conference and Exhibition Held in Boston, Massachusetts on September 15-21, 2006, The original document contains color images.

14. ABSTRACT

15. SUBJECT TERMS

16. SECURITY CLASSIFICATION OF:			17. LIMITATION OF ABSTRACT	18. NUMBER OF PAGES	19a. NAME OF RESPONSIBLE PERSON
a. REPORT	b. ABSTRACT	c. THIS PAGE			
unclassified	**unclassified**	**unclassified**	**UU**	**6**	

Our region in this study involves a cylinder centered around a bottom-mounted sensor with outer radius $d_{\max}$, a water height of H_w and an elevation beam width B_α. For this region the filter depth intervals are given by

$$z_{depth}(kd) = \sqrt{r(kd)^2 - d_{\max}^2} \;;\; kd = 1,2,...N_{depths}$$

$$r(kd) = \frac{r_{\min}}{2}(\rho^{kd} + \rho^{kd-1}), \qquad (1)$$

$$\rho = \left(\frac{r_{\max}}{r_{\min}}\right)^{1/N_{depths}},$$

$$r_{\min} = \sqrt{{d_{\max}}^2} \quad \text{and} \quad r_{\max} = \sqrt{{d_{\max}}^2 + {H_w}^2}$$

$$N_{depths} = \frac{H_w}{2d_{\max}\tan(\pi B_\alpha / 180)}.$$

More generally, depth intervals are designed to keep a constant coefficient of variation in range at the decision boundary for all filters such that model nonlinearities and relative range uncertainties are the same for all models in the filter bank when the target enters the decision region [5].

Each hypothesis model is based on an iterated-extended Kalman filter centered within its respective depth interval. The filters operate independently from the same input measurement. A Gaussian sum filter uses a weighted average to create a multi-hypothesis estimate for each update cycle; the weights are formed by normalizing the likelihoods of each depth interval.

B. Cartesian Iterated Extended Kalman Filter

A simple right hand Cartesian coordinate system defines the sensor coordinate system. The origin of the sensor coordinate system is located on the bottom of the sea floor, directly below the sensor unit's center. The *x-y* axis is level with respect to the Earth. Positive *z* indicates height above the bottom. All positions are measured in meters. The origin of the sensor coordinate system is displaced from the world coordinate system origin. The target position *(x,y,z)* in sensor coordinates is $\underline{x}_s = [\, x_s \; y_s \; z_s \,]^T$. Each EKF filter is defined in terms of relative coordinates, that is the difference between the target and the sensor. For each depth model the state vector is then

$$\underline{x} = [\, x_s \; y_s \; z_s \; \dot{x}_s \; \dot{y}_s \; \dot{z}_s \,]^T. \qquad (2)$$

The measurement vector is bearing and elevation defined by

$$\begin{bmatrix} \text{elevation (radians)} \\ \text{bearing (radians)} \end{bmatrix} = \begin{bmatrix} \alpha \\ \beta \end{bmatrix} = \begin{bmatrix} \text{Tan}^{-1}\left(\dfrac{(z_S)}{\sqrt{(x_S)^2 + (y_S)^2}}\right) \\ \text{Tan}^{-1}\left(y_s / x_s\right) \end{bmatrix}. \qquad (3)$$

A Kalman filter model is designed for each depth interval. Because the relationship between the measurements and the target position is nonlinear, an iterated-extended Kalman filter (EKF) is used to provide an appropriate recursive filtering mechanism for each hypothesis or model. Divergence can occur when the linear approximation of the relationship between the measurements and the state breaks down. To address this problem, the recursive state estimate update equation was modified by η, a line search scaling term [1] as described below:

$$\underline{\hat{x}}_{k,i+1}(+) = \underline{\hat{x}}_{k,i}(+) + \eta_{k,i}\left[\hat{x}_k(-) - \hat{x}_{k,i}(+)\right] K_{k,i} \cdot [\, \underline{z}_k - \underline{h}_k(\underline{\hat{x}}_{k,i}(+)) - H_k(\underline{\hat{x}}_{k,i}(+))(\underline{\hat{x}}_k(-) - \underline{\hat{x}}_{k,i}(+)) \,], \qquad (4)$$

$$\hat{x}_{k,0}(+) = \hat{x}_k(-)$$

where $\eta_{k,i}$ is selected to satisfy and

$$\begin{aligned} &[\underline{\hat{x}}_{k,i+1}(+) - \underline{\hat{x}}_k(-)]^T P_k^{-1}(-)[\underline{\hat{x}}_{k,i+1}(+) - \underline{\hat{x}}_k(-)] \\ &+ [\underline{z}_k - h(\underline{\hat{x}}_{k,i+1}(+))]^T R^{-1}[\underline{z}_k - h(\underline{\hat{x}}_{k,i+1}(+))] \\ &< \\ &[\underline{\hat{x}}_{k,i}(+) - \underline{\hat{x}}_k(-)]^T P_k^{-1}(-)[\underline{\hat{x}}_{k,i}(+) - \underline{\hat{x}}_k(-)] \\ &+ [\underline{z}_k - h(\underline{\hat{x}}_{k,i}(+))]^T R^{-1}[\underline{z}_k - h(\underline{\hat{x}}_{k,i}(+))] \end{aligned} \qquad (5)$$

Specifically select $\eta_{k,i}$ to be the $\max\left\{(1/2)^l,\, l = 0, 1, 2, ..., 10\right\}$ that satisfies (5). If none satisfy (5), then one assumes convergence and sets $\hat{x}_{k,i+1}(+) = x_{k,i}(+)$. One iterates from $i = 0, 1, 2, \ldots,$ *Imax* (for this study, *Imax*=10).

The filter state is a six by one column vector that indicates the target position and speed in sensor Cartesian coordinates. Targets are assumed to be moving at a constant speed so the velocity portion of the true state remains constant. The state vector (2) and the parameters of the system model are

$$\dot{\underline{x}}(t) = \begin{bmatrix} 0 & 0 & 0 & 1 & 0 & 0 \\ 0 & 0 & 0 & 0 & 1 & 0 \\ 0 & 0 & 0 & 0 & 0 & 1 \\ 0 & 0 & 0 & 0 & 0 & 0 \\ 0 & 0 & 0 & 0 & 0 & 0 \\ 0 & 0 & 0 & 0 & 0 & 0 \end{bmatrix} \underline{x}(t) + \underline{w}(t) \qquad (6)$$

where $\underline{w}(t) \sim N(0, \underline{Q}(t))$.

The state vector and error covariance matrix for each range hypothesis, $r^{(kd)}$, are initialized with a position

calculated using the first elevation and bearing measurements along with an initial range hypothesis centered about the corresponding depth interval for the respective depth mode as follows

$$\underline{\hat{x}}^{(kd)}(0) = \begin{bmatrix} \hat{x}_0 \\ \hat{y}_0 \\ \hat{z}_0 \\ \hat{\dot{x}}_0 \\ \hat{\dot{y}}_0 \\ \hat{\dot{z}}_0 \end{bmatrix} = \begin{bmatrix} r_0^{(kd)} \cos(\alpha_0)\cos(\beta_0) \\ r_0^{(kd)} \cos(\alpha_0)\sin(\beta_0) \\ r_0^{(kd)} \sin(\alpha_0) \\ 0 \\ 0 \\ 0 \end{bmatrix} \tag{7}$$

and

$$P_0 \approx A(\underline{z}_0) R\, A^T(\underline{z}_0) \ , \tag{8}$$

$$A(\underline{z}_k) = \frac{\partial \underline{g}(\underline{z}_k)}{\partial \underline{z}_k}; \ a_{i,j} = \frac{\partial g_i(\underline{z}_k)}{\partial z_j},$$

for $r_0^{(kd)}$ = hypothetical range measurement centered in corresponding depth interval (note: use actual range measurement if one is available); $R = E(\delta \underline{z}_k \delta \underline{z}_k^T)$ the measurement error covariance matrix and z_i the ith element of the measurement vector, $\underline{z}$, at time t_k.

For the results contained in this paper, the sensors are assumed to produce independent bearing and elevation and in some cases Doppler velocity and speed measurements. Hence, the measurement covariance matrix is diagonal. However, independent measurements are not a requirement. The diagonal elements of the covariance matrix have units of radians^2, radians^2, meters^2 per second^2 and meters^2 per second^2. After the P matrix is initialized using this approach, it should be checked to ensure that it is positive definite.

C. Multi-hypothesis track estimate

The MHEKF track is recursively updated using the independent filter bank outputs at each filter depth in combination with a multi-hypothesis test. Upon every measurement each filter in the bank is updated independently. For each filter track, the MHEKF then forms a composite track based on a weighted average of all depths within the corresponding track; the weights are based on the likelihood of each track. Figure 1 gives the logic structure for the multi-hypothesis filter bank. In the case of multiple targets the composite track is used to assign each target to an MHEKF filter bank.

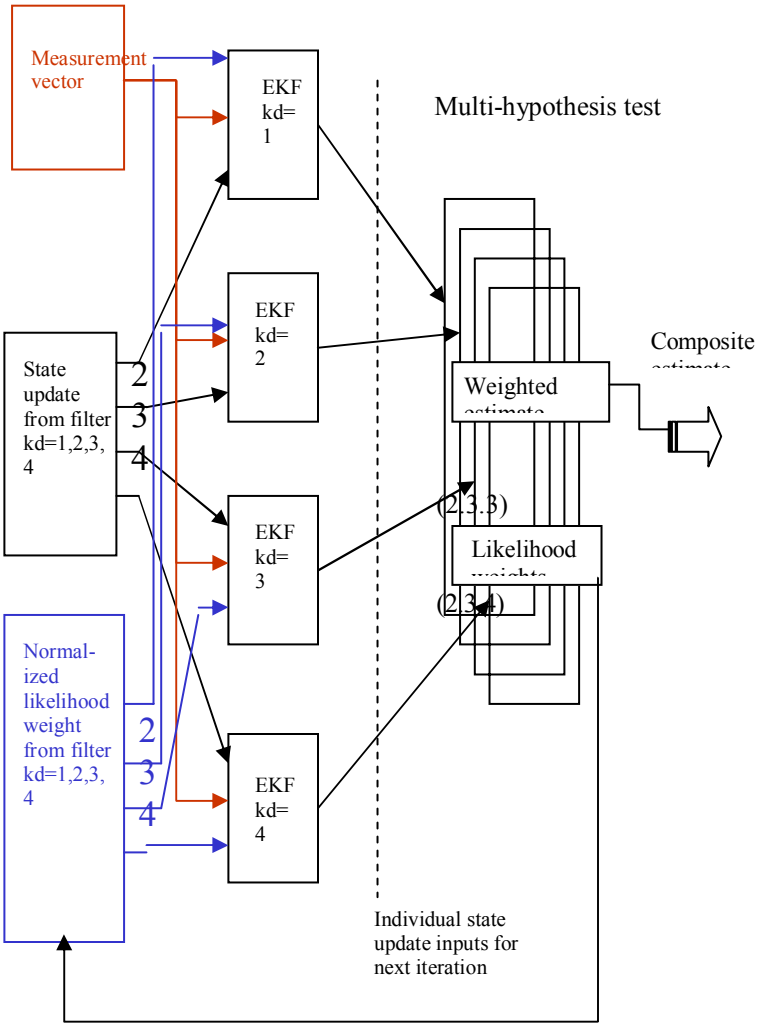

Figure 1 Multi-hypothesis filter bank logic structure.

The multi-hypothesis estimate uses the normalized likelihood from each filter depth-mode output, or each EKF, to recursively update the target track [3]. Each filter model is independently updated. The combined state estimate at each update cycle uses a Gaussian sum filter.

For the Cartesian EKF model defined in Section *B.* the normalized likelihood weight for each depth mode expresses as

$$w_t^{(kd)} = \ell_t^{(kd)} \Big/ \sum_i \ell_t^{(i)} \tag{9}$$

where

$$\ell_t^{(kd)} = \frac{\exp\left(\frac{1}{2}(\underline{z}_t - h(\underline{\hat{x}}^{(kd)}_{t/t-1})^T \left[H_t^{(kd)} P^{(kd)}_{t/t-1} (H_t^{(kd)})^T + R_i\right]^{-1} (\underline{z}_t - h(\underline{\hat{x}}^{(kd)}_{t/t-1})\right)}{\sqrt{H_t^{(kd)} P^{(kd)}_{t/t-1} (H_t^{(kd)})^T + R_i}}$$

for $\underline{z}_t = [\alpha_t \quad \beta_t]^T$ the measurement vector at time t,

$$h(\underline{\hat{x}}) = \begin{bmatrix} \sqrt{(x_S)^2 + (y_S)^2 + (z_S)^2} \\ \mathrm{Tan}^{-1}\left(\dfrac{(z_S)}{\sqrt{(x_S)^2 + (y_S)^2}} \right) \\ \mathrm{Tan}^{-1}\left(y_S / x_S \right) \\ \dfrac{(x_S)\dot{x} + (y_S)\dot{y} + (z_S)\dot{z}}{\sqrt{(x_S)^2 + (y_S)^2 + (z_S)^2}} \\ \sqrt{(\dot{x}_S)^2 + (\dot{y}_S)^2 + (\dot{z}_S)^2} \end{bmatrix} = \begin{bmatrix} \text{range (meters)} \\ \text{elevation (radians)} \\ \text{bearing (radians)} \\ \text{Doppler velocity (meters/sec)} \\ \textit{Speed} \text{ (meters/sec)} \end{bmatrix}, \quad (2.4.3)$$

and

$$H(\underline{\hat{x}}_{k,i}(+)) = \left. \frac{\partial \underline{h}(\underline{x}(t_k))}{\partial \underline{x}(t_k)} \right|_{\underline{x}(t_k) = \underline{\hat{x}}_{k,i}(+)} . \quad (2.4.4)$$

The combined state estimate and covariance matrix for the MHEKF are formed from the normalized likelihood weights defined (9) and the respective updates from each EKF in the filter bank using the formulas below

$$\hat{x}_{t/t} = \sum_{kd=1}^{N_{depths}} w_t^{(kd)} \hat{x}^{(kd)}{}_{t/t-1} , \quad (10)$$

$$P_{t/t} = \sum_{kd=1}^{N_{depths}} w_t^{(kd)} [P_{t/t}^{(kd)} + (\hat{x}_{t/t}^{(kd)} - \hat{x}_{t/t})(\hat{x}_{t/t}^{(kd)} - \hat{x}_{t/t})^T] \quad (2.4.5)$$

.

A counter is inserted in the filter logic such that if the *z* coordinate, or depth, of the sub-track estimate for a given EKF is consistently out of bounds for that depth filter model or if the likelihood estimate remains below a threshold then the filter is automatically removed and a new threshold value for the remaining depth filter models is recomputed. The threshold is originally set as a function of the number of depth modes set during the range parameterization process. Any additional target class information can be used to refine the threshold settings.

III. TRACKING ERROR ANALYSIS

Test cases were run over varying track conditions. In the illustrated examples the decision region was defined to be a cylinder in the water column with a radius of 500 meters and an inner radius of 300 meters. One goal of the MHEKF is to generate a 'go active' decision signal when, within a prescribed confidence interval, the MHEKF detects a target in this decision region cylinder.

Figure 2 illustrates the test tracks in the x-y plane. The test tracks were generated using straight-and-level trajectories across numerous depths, heading angles and closest points of approach (CPA). The sensor is centered in the decision cylinder, at the bottom of the water column. An action decision is made when the target along a given track is located within the inner and outer radius walls of the cylinder.

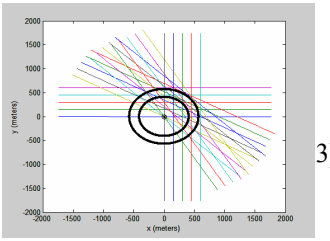

Figure 2. Target tracks viewed in x-y plane.

The polar description for the above tracks for a target at a depth of z=280 is given in Figure 3. For a target at that depth the range between the sensor and the target when the target enters the decision region is R=573 meters. Recall, range measurements will not be available.

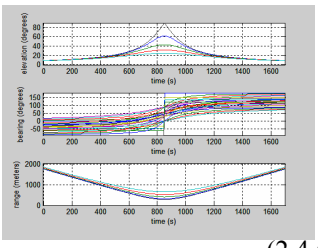

Figure 3. Range, elevation and bearing coordinates for target tracks for z=280.

Figures 4a-d give the multi-hypothesis target track estimates for different values of CPA. The RMSE error bar spreads for each track illustrate the error variance centered about the mean estimate calculated over multiple Monte Carlo runs for that track. The black line is the true track A CPA of zero indicates the target goes directly over the sensor. When the target tracks are outside the decision region but the error variance bar is inside the decision region, as in Figure 4d, a call is still likely to be made.

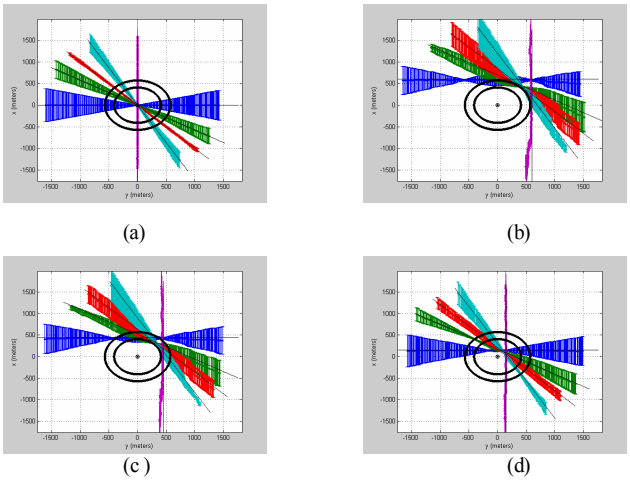

Figure 4 RMSE error bar spreads for the MHEKF position estimates. (a) CPA=0 (b) CPA=150 (c) CPA=450 (d) CPA=600.

Figures 5a-d give performance results over all test tracks taken over various values of CPA, target depth, velocity and heading. The plots give error statistics as a

function of track for range, elevation, bearing and depth estimates of target position at the precise point of a 'go active' decision. The stars locate the mean error over multiple Monte Carlo runs for a specific track and the bars give the error variance for that track. The tracks are numbered as follows in groups of five corresponding to the headings in degrees of [0 30 45 60 90] and tracks 1-5 are for a CPA of 0; tracks 6-10 are for a CPA of 150; tracks 11-15 are for CPA=300; tracks 16-20 are for CPA=450; and tracks 21-25 are for CPA=600. For example in Figure5(a) the bar corresponding to track number 4 (CPA=450 and a heading of 45 degrees) indicates a mean error of 20 meters off from the true range of 573 meters and an RMS error of 43 meters

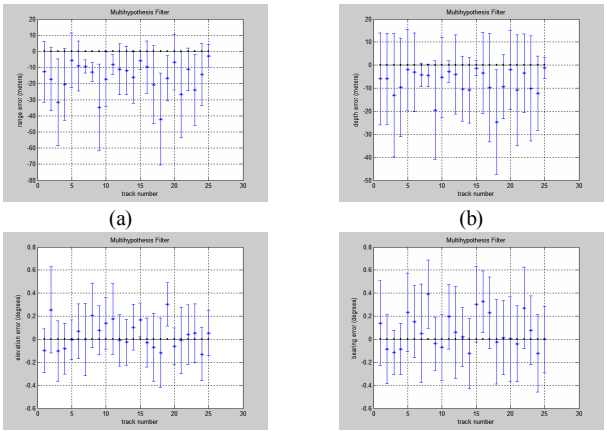

Figure 5. Error analysis for multi-hypothesis tracking filter.

IV. PERFORMANCE RESULTS

Multiple runs were made to examine tracking performance of the multi-hypothesis tracker. Tracking success was defined as a proper 'go active' call inside the decision boundary and positioning to within 20 percent of the true track. Table 1 gives a breakdown of the run parameters

TABLE 1

VARIABLE RUN PARAMETERS USED IN TRACKER TESTING

	Water depth 300 meters	Water depth 200 meters
Target height above sonar (Meters)	Surface, 280, 200, 160, 80	Surface, 160, 80
Target speed (knots)	4, 10	4
Target CPA (Meters)	0,150,300,450,600	0,150,300,450,600
Target headings (Degrees)	0, 30, 45, 60, 90	0, 30, 45, 60, 90

Overall about a 78% success rate was achieved from elevation and bearing measurements coupled with bounding of the velocity vectors with a 20-knot constraint. Inclusion of speed or Doppler information into the EKF equations raised the level to about a 95% success rate.

A Pareto analysis was completed on the control data taken over tracking runs given elevation and bearing measurements and bounded velocity vectors. Figure 6 gives the corresponding Pareto diagram for the tracking errors.

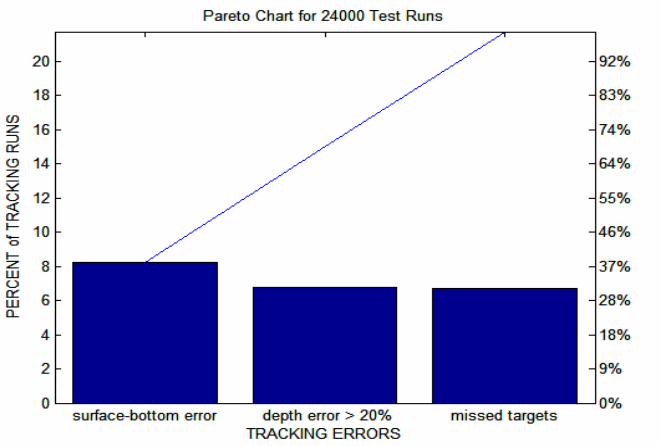

Figure 6. Pareto chart for 24000 test runs with bounding of the velocity vectors.

Tracking errors were broken into one of three categories. The first and largest category was tracking failures that occurred when the tracker locked onto a slow moving bottom track for a fast moving surface target or vice versa. This occurs when the velocity bounds in the filters are large due to inadequate target class or velocity information and the rate of change in the bearing and elevation are the same for the two filter depth modes. Additional target class or velocity information is required to eliminate this problem. Category 2 comprised all other tracking failures that arose from poor positioning. These were due mostly to improper thresholding and weighting in the multi-hypothesis stage of the tracker resulting from inadequate target information. The final category consists of targets which were either missed completely or not given a 'go active' while in the decision region. The dominant set of targets here were targets low in the water column that had already moved past CPA and exited the decision region before the tracker initiated a 'go active' call. The missed calls occurred most often when the tracker locked onto a near surface track for a deep submerged target. With proper target class or velocity information the tracker would be able to eliminate the near surface track as an unlikely scenario because the high rate of change in elevation coupled with the long ranges of the surface track would not fall within the velocity variance.

Figure 7 compares run results for different levels of target velocity information. Each bar indicates the percentage of tracking errors that occurred over runs within the specified categories. Run results are broken down into three categories: elevation and bearing measurements with velocity bounding on the estimate equations; elevation, bearing and speed measurements input to the estimation; and elevation, bearing and Doppler measurements. Notice the inclusion of speed or Doppler directly into the state

estimate equations lowers the percentage of tracking failures from greater than 20 percent to on the order of 5 percent.

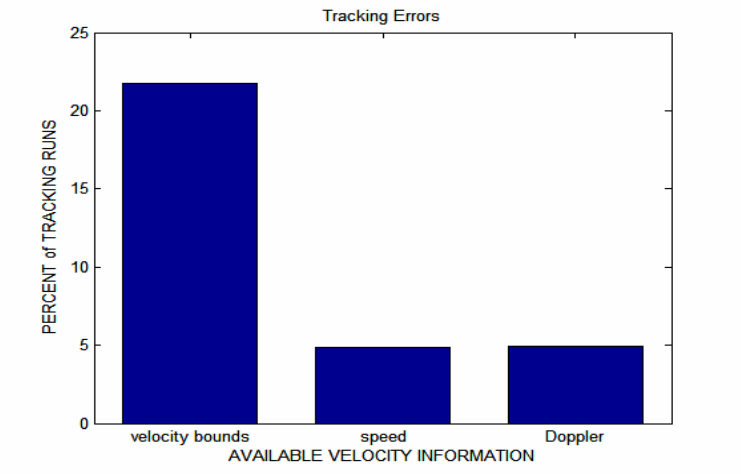

Figure 7. Relative tracking error for different levels of velocity information.

V. DISCUSSION AND CONCLUSIONS

We have developed and implemented an iterated-extended Kalman filter for target tracking. Problems associated with missing range measurements have been addressed by implementing a multi-depth mode tracker. Range measurements are artificially created by initializing multiple Kalman filters at pre-determined depths. Assigning a depth to an elevation/bearing pair uniquely solves the *x, y, z* target position initialization problem. Hence, an elevation/bearing pair will result in *Nd* Kalman filters - one at depth 1, one at depth 2, …, and one at depth *Nd*. A multi-hypothesis estimation scheme is used to determine the target track from the *Nd* Kalman filters. Target related bounding of the velocity vectors is necessary in the absence of range information. Velocity or speed information is needed to eliminate track ambiguities.

Track ambiguity arises when the tracker is expected to distinguish fast moving targets on the surface from slow moving targets at depth unless target class or velocity information is entered into the multi-hypothesis decision logic. In addition to bounding the velocity vectors for each filter depth model, target information must be coupled to the threshold and counter parameters in the Gaussian sum filter. Performance is inversely related to target velocity.

To prevent filter divergence, a scaling term, η, has been included in the recursive state estimate update defined in (4). During the recursive state estimate update, η is initialized to 1.0. If the line search inequality in (5) is not satisfied, η is then repeatedly halved until the inequality is satisfied. If the inequality is still not satisfied after ten attempts, η is then set to zero. This line search procedure ensures that the iterated Kalman filter converges. Equations (4) and (5) detail this procedure.

A Pareto analysis of the run results indicate that considerable performance gains are achieved when either speed or Doppler measurements are available to the tracker. Future analysis would involve modification of the propagation equations for long lag between samples, a broader sensitivity analysis, and a detailed analysis of variance.

REFERENCES

[1] J.C. Hyland, *An Iterated-Extended Kalman Filter Algorithm for Tracking Surface and Sub –Surface Targets,* OCEANS 2003.

[2] *Use of Least Squares for a Nonlinear Problem: Bearings Only Target Motion Analysis*, Chapter 3, Section 3.7, pp161-172, S. S. Blackman, *Multiple Target Tracking with Radar Applications*, Artech House, Inc., Norwood, Massachusetts, 1986

[3] R. Karlsson and F. Gustafsson, *Recursive Bayesian Estimation – Bearings-only Applications, In Review for IEE Proceedings Radar, Sonar and Navigation, special issue on target tracking: Algorithms and Applications.*

[4] R. Karlsson and F. Gustafsson, *Range estimation using angle-only target tracking with particle filters,* Proceedings of the American Control Conference, Arlington, VA, June 25-27, 2001, pp. 3743-3748

[5] T.R Kronhamn, *Bearings-only target motion analysis based on a multihypothesis Kalman filter and adaptive ownship motion control,* IEE Proceedings Radar, Sonar and Navigation, Vol. 145, No. 4, August 1998.

[6] N. Peach, *Bearings-only tracking using a set of range-parameterized extended Kalman filters,* IEE Proceedings Control Theory Applications, Vol. 142, No. 1, January 1995.

[7] S.S. Blackman, *Multiple Target Tracking with Radar Applications*, Artech House, Inc., Norwood, Massachusetts, 1986.

[8] R.B. Blackman and J.W. Tukey, "The Measurement of Power Spectra: From the Point of View of Communications Engineering," Dover Publications, Inc., NY, 1959, Chapter 9, pp. 21-22.

[9] Gelb, J. F. Kasper, Jr., R. A. Nash, Jr., C. F. Price, and A. A. Sutherland, *Applied Optimal Estimation*, The M.I.T. Press, Cambridge, Massachusetts, 1974.

[10] J.C. Hyland and G.J. Dobeck, "Estimating Sonar Target Positions with an Extended Kalman Filter, CSS TN 1122-92, Coastal Systems Station, Panama City, Florida, October 1992.